



## Original Contribution

## Scope and limitations of the TEMPO/EPR method for singlet oxygen detection: the misleading role of electron transfer

Giacomo Nardi<sup>a</sup>, Ilse Manet<sup>b</sup>, Sandra Monti<sup>b</sup>, Miguel A. Miranda<sup>a</sup>, Virginie Lhiaubet-Vallet<sup>a,\*</sup><sup>a</sup> Instituto de Tecnología Química UPV-CSIC, Universitat Politècnica de València, 46022 Valencia, Spain<sup>b</sup> Istituto per la Sintesi Organica e la Fotoreattività, Consiglio Nazionale delle Ricerche, 40129 Bologna, Italy

## ARTICLE INFO

## Article history:

Received 25 June 2014

Received in revised form

19 August 2014

Accepted 20 August 2014

Available online 16 September 2014

## Keywords:

EPR

Photosensitizer

Singlet oxygen

TEMPO

Time-resolved near-infrared emission

Free radicals

## ABSTRACT

For many biological and biomedical studies, it is essential to detect the production of  $^1\text{O}_2$  and quantify its production yield. Among the available methods, detection of the characteristic 1270-nm phosphorescence of singlet oxygen by time-resolved near-infrared (TRNIR) emission constitutes the most direct and unambiguous approach. An alternative indirect method is electron paramagnetic resonance (EPR) in combination with a singlet oxygen probe. This is based on the detection of the TEMPO free radical formed after oxidation of TEMP (2,2,6,6-tetramethylpiperidine) by singlet oxygen. Although the TEMPO/EPR method has been widely employed, it can produce misleading data. This is demonstrated by the present study, in which the quantum yields of singlet oxygen formation obtained by TRNIR emission and by the TEMPO/EPR method are compared for a set of well-known photosensitizers. The results reveal that the TEMPO/EPR method leads to significant overestimation of singlet oxygen yield when the singlet or triplet excited state of the photosensitizer is efficiently quenched by TEMP, acting as electron donor. In such case, generation of the  $\text{TEMP}^{+\bullet}$  radical cation, followed by deprotonation and reaction with molecular oxygen, gives rise to an EPR-detectable TEMPO signal that is not associated with singlet oxygen production. This knowledge is essential for an appropriate and error-free application of the TEMPO/EPR method in chemical, biological, and medical studies.

© 2014 Elsevier Inc. All rights reserved.

Singlet oxygen (molecular oxygen in the  $^1\Delta_g$  state, or  $^1\text{O}_2$ ) is one of the most important “reactive oxygen species.” Its reactions include oxidation of lipids [1,2], proteins [3–5], and nucleic acids [6–8], which may trigger biological damage. This reaction cascade can lead to undesired adverse effects, such as drug-induced phototoxicity [9,10], but can also be exploited to produce beneficial effects as in photodynamic therapy [11,12].

Production of  $^1\text{O}_2$  by a photosensitizer is a classical example of photoinduced energy transfer: after absorption of light, the photosensitizer reaches its singlet excited state and subsequently crosses to its triplet excited state. Then, the triplet ground state of molecular oxygen is promoted to the  $^1\Delta_g$  state through triplet–triplet energy transfer [13].

**Abbreviations:** ACN, acetonitrile; BAHA, tris(4-bromophenyl)aminium hexachloroantimonate; BP, benzophenone; CBZ, carbazole; EPR, electron paramagnetic resonance; LFP, laser flash photolysis; NP, naphthalene; PET, photoinduced electron transfer; PN, phenalenone; RB, rose Bengal; TEMP, 2,2,6,6-tetramethylpiperidine; TEMPO, 2,2,6,6-tetramethyl-1-piperidinyloxy; TRNIR, time-resolved near infrared

\* Corresponding author.

E-mail address: [lvirgini@itq.upv.es](mailto:lvirgini@itq.upv.es) (V. Lhiaubet-Vallet).

For many biological and biomedical studies, it is essential to detect the production of  $^1\text{O}_2$  and quantify its production yield. Among the available methods, detection of the characteristic 1270-nm phosphorescence of singlet oxygen by time-resolved near-infrared (TRNIR)<sup>1</sup> emission constitutes the most direct and unambiguous proof [14,15]. However, the required equipment is not always available in biochemical laboratories.

An alternative indirect method that has been widely applied is electron paramagnetic resonance (EPR) in combination with a  $^1\text{O}_2$  probe. Upon reaction with  $^1\text{O}_2$ , the trapping molecule gives rise to a detectable spin-active species with a distinctive line pattern. Thus, oxidation of TEMP (2,2,6,6-tetramethylpiperidine) by singlet oxygen yields the TEMPO (2,2,6,6-tetramethyl-1-piperidinyloxy) free radical easily detected by EPR (Fig. 1) [16]. Although the TEMPO/EPR method has been widely employed [17–25], a systematic investigation of the scope and limitations of this technique has never been performed. For instance, amines are widely known for their ability to quench excited states, so a probable source of artifacts may be the interaction between the excited photosensitizer and TEMP [26–29]. The aim of the present study was to compare the results obtained for the detection and quantification of singlet oxygen by means of the direct method (TRNIR emission)

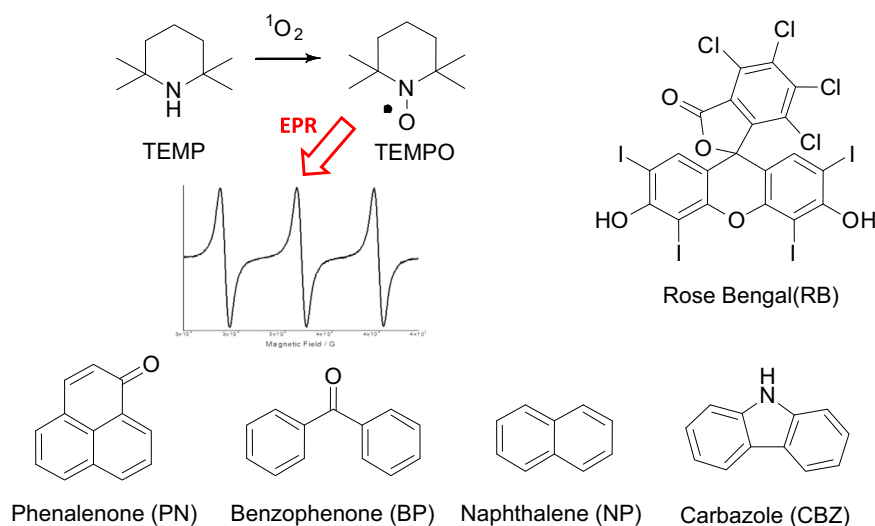


Fig. 1. Structure of the molecules involved in the study and EPR signal of the TEMPO radical.

and the indirect  $^1\text{O}_2$  trapping mode (TEMPO/EPR method), using a set of well-known photosensitizers. The basis of the TEMPO method and the chemical structure of the selected photosensitizers are shown in Fig. 1. The results obtained reveal that the EPR method leads to significant overestimation of singlet oxygen production when the singlet or triplet excited state of the photosensitizers is efficiently quenched by TEMP, acting as electron donor.

## Materials and methods

### Chemicals

TEMP, tris(4-bromophenyl)aminium hexachloroantimonate (BAHA), phenalenone (PN), benzophenone (BP), naphthalene (NP), carbazole (CBZ), rose Bengal (RB), and acetonitrile (ACN) were from Sigma-Aldrich. TEMP was freshly distilled at 152 °C before use.

### Absorption and fluorescence spectra

UV–Vis absorption spectra were recorded on a commercial spectrophotometer ( $\lambda 650$ ; PerkinElmer). Fluorescence spectra were measured using 1-nm steps and 0.5-s dwell time, at right-angle detection (FLSP920; Edinburgh Instruments). Slits were kept narrow to 1 nm for excitation and 1 or 2 nm for emission; where necessary, a cutoff filter was used. All the measurements were carried out at 295 K in quartz cuvettes with a path length of 1 cm. The fluorescence spectra were obtained for air-equilibrated solutions with  $A < 0.1$  over the whole absorption range to avoid inner filter effects and reabsorption of emission. Quenching of CBZ and NP fluorescence intensity by TEMP upon excitation at 331 and 278 nm, respectively, was performed by adding increasing amounts of TEMP to the solution. For NP measurements, the fluorescence intensities were corrected for the inner filter effect due to absorption of TEMP at 278 nm. The following equation was used to determine  $K_{sv}$ , the Stern–Volmer quenching constant:

$$F_0/F = 1 + K_{sv}[Q]. \quad (1)$$

In Eq. (1),  $F_0$  and  $F$  are the fluorescence intensities, respectively, in the absence and presence of the quencher Q;  $[Q]$  is the quencher concentration (M); and  $K_{sv}$  is the Stern–Volmer constant. The bimolecular quenching rate constant  $k_q$  ( $\text{M}^{-1} \text{s}^{-1}$ ) was obtained dividing  $K_{sv}$  by the fluorescence lifetime.

### Fluorescence lifetimes

Fluorescence decay was measured in air-equilibrated solutions with a time-correlated single-photon counting apparatus (IBH 5000F) equipped with a TBX picosecond photon detection module. A nano-LED pulsed excitation source at 331 and 278 nm was used and the emission was collected at right angle at 341 or 320 nm using a long-pass cutoff filter at 305 nm. Fluorescence decay profiles were fitted using a monoexponential function of the decay analysis software DAS6 provided by the manufacturer with deconvolution of the instrumental response function.

### Laser flash photolysis measurements

The beam of a pulsed Nd:YAG laser, operating at 532 or 355 nm (20 ns FWHM, 2 Hz, 2.7 mJ/pulse), was suitably shaped to pass through a 3-mm-high and 10-mm-wide rectangular window and provide a fairly uniform energy density of 9 mJ/cm<sup>2</sup> incident onto the sample cell. A front portion of 2-mm depth of the excited solution was probed at right angle, the useful optical path for analyzing light being 1 cm. All transient spectra were recorded with 3 ml of sample solutions in  $1 \times 1\text{-cm}^2$  quartz cells; when specified ACN solutions were bubbled for 10 min with Ar before data acquisition. The absorbance of the samples was kept in the range 0.30–0.40 at the laser wavelength. Stock solutions of the quenchers were prepared, so that addition of microliter volumes to the sample cell allowed us to obtain the appropriate quencher concentration.

The bimolecular rate constant  $k_q$  ( $\text{M}^{-1} \text{s}^{-1}$ ) for quenching of the triplet states was calculated from the slope of linear plots of the observed triplet decay rate constant  $k_{obs}$  ( $\text{s}^{-1}$ ) versus the quencher concentration, applying Eq. (2),

$$k_{obs} = k_0 + k_q[Q], \quad (2)$$

where  $k_0$  is the triplet decay rate constant in the absence of quencher and  $[Q]$  is the quencher molar concentration (M).

### Singlet oxygen TRNIR emission measurements

The pulse of a Nd:YAG laser, operating at 355 or 266 nm (20-ns FWHM), was used for excitation of the samples dissolved in air-equilibrated acetonitrile. A preamplified (low impedance) Ge photodiode (Applied Detector Corp., Model 403HS, time resolution 300 ns), cooled at 77 K and equipped with a 5-mm-thick

AR (anti-reflection)-coated silicon metal filter with wavelength pass  $> 1.1 \mu\text{m}$  and an interference filter at  $1.27 \mu\text{m}$ , was used to measure emission of singlet oxygen at  $1270 \text{ nm}$  in right-angle geometry. The photodiode output current was fed into a digital oscilloscope. All measurements were made at room temperature in 1-cm-path length quartz cuvettes. The absorbance of the samples was 0.30 at the laser wavelength. The singlet oxygen quantum yield ( $\phi_{\Delta}$ ) was determined using phenalenone in acetonitrile ( $\phi_{\Delta}^{\text{ref}} = 0.95$ ) as reference [30]. Singlet oxygen formation quantum yield was calculated from the slope of linear plots representing signal intensity at zero time versus laser pulse energy according to the equation  $\phi_{\Delta} = \phi_{\Delta}^{\text{ref}}(I_{\text{sample}}/I_{\text{ref}})$ , where  $I_{\text{sample}}$  is the emission intensity for the sample at pulse end,  $I_{\text{ref}}$  is the emission intensity for the reference, and  $\phi_{\Delta}^{\text{ref}}$  is the quantum yield of singlet oxygen formation of the reference.

#### EPR trapping measurements

The EPR signal of the free radical TEMPO ( $g = 2.0060$ ,  $a_N = 17.3 \text{ G}$ ) generated by the reaction of singlet oxygen with TEMPO was recorded [31]. The measurements were performed in a Wildman Suprasil/aqueous quartz-ware flat cell (volume  $150 \mu\text{l}$ , length  $60 \text{ mm}$ ) with a Bruker EMX 10/12 EPR spectrometer, using the following parameters: microwave power,  $20 \text{ mW}$ ; modulation amplitude,  $1.0 \text{ G}$ ; and modulation frequency,  $100 \text{ kHz}$ .

Aerated ACN solutions of  $50 \text{ mM}$  TEMP containing a photosensitizer, with an absorbance of  $0.4$  at  $280 \text{ nm}$ , were irradiated using the light produced by a Microbeam system (Model L-201), including a  $150\text{-W}$  xenon lamp coupled with a monochromator (Model 101); EPR spectra were recorded at various irradiation times. The singlet oxygen quantum yield ( $\phi_{\Delta}$ ) was determined using phenalenone in acetonitrile ( $\phi_{\Delta}^{\text{ref}} = 0.95$ ) as reference [30]. Singlet oxygen formation was calculated from the slope of the plots of signal area versus irradiation time according to the equation  $\phi_{\Delta} = \phi_{\Delta}^{\text{ref}}(x_{\text{sample}}/x_{\text{ref}})$ , where  $x_{\text{sample}}$  is the coefficient of linear fit for the sample,  $x_{\text{ref}}$  is the coefficient of linear fit for the reference, and  $\phi_{\Delta}^{\text{ref}}$  is the quantum yield of singlet oxygen formation of the reference.

In the case of BAHA oxidation, EPR spectra of aerated ACN solutions of  $50 \text{ mM}$  TEMP were recorded before and after addition of  $0.1$  BAHA equivalents.

#### Photoinduced electron transfer

According to Rehm and Weller [32] the free energy change  $\Delta G$  for electron transfer is expressed by  $\Delta G = E_{\text{ox}} - E_{\text{red}} - E^* + C$ , where  $E_{\text{ox}}$  is the oxidation potential of the donor,  $E_{\text{red}}$  is the reduction potential of the ground-state acceptor,  $E^*$  is the energy of the acceptor excited state, and  $C$  is a coulombic term accounting for the electrostatic attraction of the produced ions. Neglecting the  $C$  term,  $\Delta G$  was calculated using the following values for the potentials:  $E_{\text{ox}}$  (TEMP) =  $1.0 \text{ V}$  and  $E_{\text{red}} = -1.2, -1.3, -2.6$ , and  $-1.8 \text{ V}$  vs SCE (Saturated Calomel Electrode) for PN [33], BP [20], NP [34], and CBZ [35], respectively. In the cases of PN [36] and BP [20], the lowest triplet excited state energy was considered for  $E^*$ , with values of  $220$  and  $292 \text{ kJ mol}^{-1}$ , respectively, whereas this parameter was associated with the singlet manifold for NP [34] and CBZ [37], using values of  $377$  and  $344 \text{ kJ mol}^{-1}$ , respectively.

## Results and discussion

#### Determination of singlet oxygen quantum yield by TRNIR emission or TEMPO/EPR

Singlet oxygen quantum yields ( $\phi_{\Delta}$ ) were determined for each photosensitizer by both a direct method (TRNIR emission) and an

indirect method (TEMPO/EPR), by comparison with phenalenone ( $\phi_{\Delta} = 0.95$ ) [30] (Fig. 2). The values obtained are reported in Table 1. The results of the TRNIR direct method are in accordance with literature values [37–39]. However, the quantum yield of benzophenone evaluated by the indirect method TEMPO/EPR was significantly higher. This result is somewhat intriguing as, upon addition of  $50 \text{ mM}$  TEMP to the benzophenone solution, the direct TRNIR emission measurement led to nearly zero quantum yield (Figs. 2B and 3A).

#### Effect of added TEMP on singlet oxygen detection by TRNIR

To investigate the direct effect of TEMP on  $^1\text{O}_2$  production, TRNIR emission measurements were performed with photosensitizers in

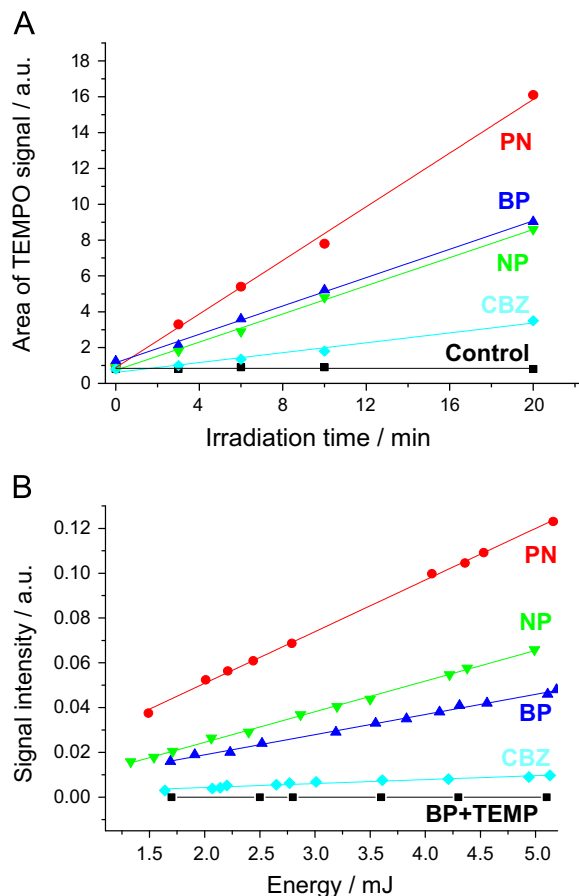


**Fig. 2.** Quantification of  $^1\text{O}_2$  formation for aerated acetonitrile solutions of photosensitizers. (A) Area of TEMPO signal in EPR as a function of irradiation time at  $280 \text{ nm}$ ,  $A_{280} = 0.4$  (control: ACN solution of  $50 \text{ mM}$  TEMP). (B) Initial intensity of  $^1\text{O}_2$  TRNIR emission as a function of  $266\text{-nm}$  laser energy,  $A_{266} = 0.3$ ; BP + TEMP, a solution of BP and  $50 \text{ mM}$  TEMP.

**Table 1**  
Singlet oxygen quantum yield of each photosensitizer.

	$\phi_{\Delta}/\text{TRNIR}^a$	$\phi_{\Delta}/\text{EPR}$
Phenalenone	0.95 <sup>b</sup>	0.95 <sup>b</sup>
Benzophenone	0.35 (0.35) <sup>c</sup>	0.50
Naphthalene	0.56 (0.5) <sup>d</sup>	0.50
Carbazole	0.15 (0.17) <sup>e</sup>	0.21

<sup>a</sup> Literature values are in parentheses.

<sup>b</sup> Reference, see Ref. [30].

<sup>c</sup> From Ref. [39].

<sup>d</sup> From Ref. [38].

<sup>e</sup> From Ref. [37].

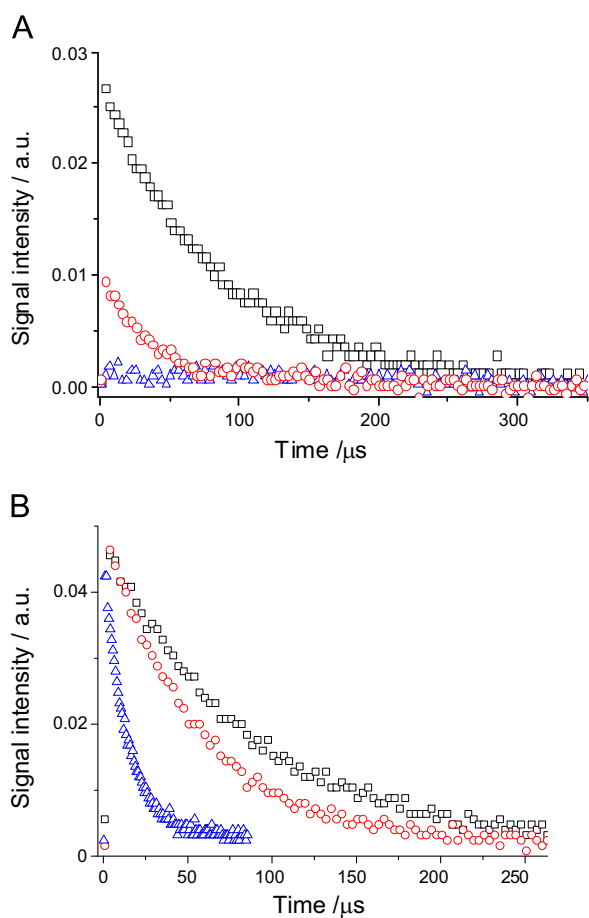


**Fig. 3.** Luminescence decay of <sup>1</sup>O<sub>2</sub> at 1270 nm in aerated ACN solution of (A) BP or (B) PN with 0 (□), 5 (○), or 50 mM (Δ) TEMP. Incident 355-nm laser energy: 3.65 mJ/pulse,  $A_{355} = 0.3$ .

the presence of increasing amounts of TEMP. As shown in Fig. 3, in the absence of TEMP the <sup>1</sup>O<sub>2</sub> lifetime was 85 μs using either phenalene or benzophenone, in accordance with the literature value [40]. Addition of TEMP to the solution had different consequences depending on the photosensitizer: in the case of phenalene TEMP acted as a poor quencher, shortening the <sup>1</sup>O<sub>2</sub> lifetime with  $k_q = 1.3 \times 10^6 \text{ M}^{-1} \text{ s}^{-1}$  [41], a result consistent with literature data; in the case of BP, in addition to lifetime shortening, TEMP was able to knock out the formation of <sup>1</sup>O<sub>2</sub> (Fig. 3A). This observation indicates that there is an interaction between TEMP and the precursor of <sup>1</sup>O<sub>2</sub>, namely the excited triplet state of BP. In the case of PN, addition of TEMP did not influence the initial TRNIR signal intensity of <sup>1</sup>O<sub>2</sub>, but affected the <sup>1</sup>O<sub>2</sub> lifetime (Fig. 3B).

#### Quenching of photosensitizer excited states by TEMP

In view of the effects produced by addition of TEMP on the <sup>1</sup>O<sub>2</sub> TRNIR signal, the triplet–triplet transient absorption of the photosensitizers was studied by laser flash photolysis in the presence of TEMP (see Supplementary Figs. S2–S4). In the case of BP, triplet quenching by TEMP was observed with rate constant  $k_q = 1.5 \times 10^9 \text{ M}^{-1} \text{ s}^{-1}$ , in accordance with the literature [42,43]. In the case of PN, although TEMP was also able to deactivate the triplet excited state, the measured rate constant was 2 orders of magnitude lower ( $k_q = 8.3 \times 10^6 \text{ M}^{-1} \text{ s}^{-1}$ ). In contrast, the rate constants for triplet quenching by oxygen are very similar for the two ketones (ca.  $2.5 \times 10^9 \text{ M}^{-1} \text{ s}^{-1}$ ). Taking into account the competition between TEMP and O<sub>2</sub>, as well as the  $k_q$  values and the TEMP and O<sub>2</sub> concentrations (50 and 1.9 mM, respectively),

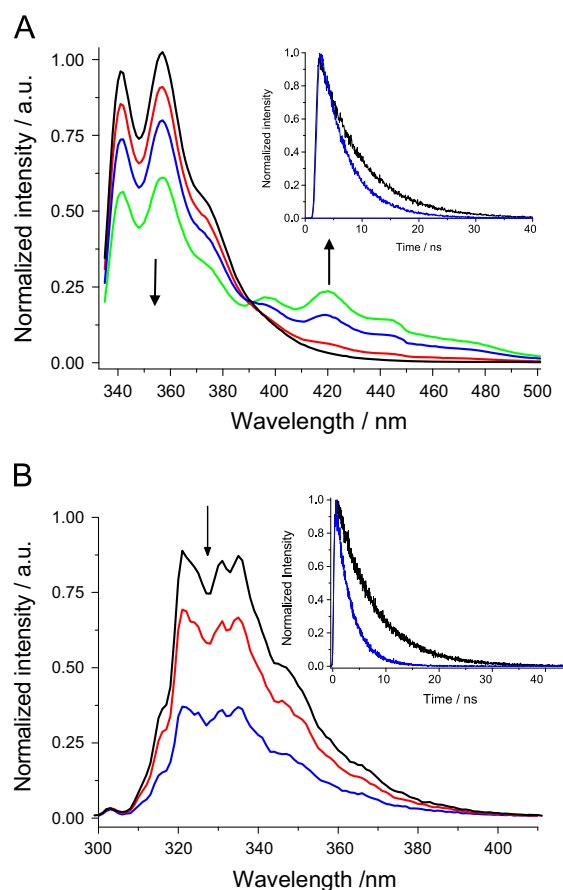


**Fig. 4.** (A) Steady-state fluorescence spectra of CBZ in aerated ACN solution with increasing amounts of TEMP. [CBZ]  $3.5 \times 10^{-5} \text{ M}$ ,  $\lambda_{\text{ex}}$  331 nm. [TEMP] 0 (black), 10 (red), 50 (blue), 100 mM (green). Inset: decay of CBZ at 341 nm in aerated ACN solution with 0 (black) and 100 mM TEMP (blue). (B) Steady-state fluorescence spectra of NP in aerated ACN solution with increasing amounts of TEMP. [NP]  $2.3 \times 10^{-6} \text{ M}$ ,  $\lambda_{\text{ex}}$  278 nm. [TEMP] 0 (black), 10 (red), 50 mM (blue). Inset: decay of NP at 320 nm in aerated ACN solution with 0 (black) and 50 mM TEMP (blue).

more than 90% of triplet BP is quenched by TEMP, whereas more than 90% of triplet PN is quenched by O<sub>2</sub> under the conditions employed. This fact explains the difference between BP and PN in the singlet oxygen formation yields upon TEMP addition.

As regards NP and CBZ, weak intensity of the LFP signals makes their triplet states barely detectable in the presence of TEMP (for example, Supplementary Fig. S4); this was attributed to a scarce population of the triplet states caused by quenching of the precursor singlet excited states. To check this hypothesis, the emission signals of NP and CBZ were monitored in the presence of TEMP. The results for CBZ are shown in Fig. 4A; they reveal a marked decrease in the fluorescence intensity concomitant with the growth of a new structured emission band with peaks at 400, 420, 450, and 470 nm. This type of long-wavelength emission has been previously observed in the presence of amines and attributed to charge transfer in the excited state (excited CBZ carbanion and/or exciplex formation) [44]. The  $k_q$  determined by means of steady-state and time-resolved emission measurements were  $9.1 \times 10^8$  and  $6.7 \times 10^8 \text{ M}^{-1} \text{ s}^{-1}$ , respectively (Supplementary Fig. S5). The difference between the two values suggests the contribution of static quenching, probably due to formation of a ground-state complex.

Likewise, the singlet excited state of NP was quenched by TEMP (Fig. 4B); the rate constant obtained from steady-state fluorescence ( $k_q = 1.9 \times 10^9 \text{ M}^{-1} \text{ s}^{-1}$ , Supplementary Fig. S6) was similar to that resulting from time-resolved fluorescence ( $k_q = 2.0 \times 10^9 \text{ M}^{-1} \text{ s}^{-1}$ ), indicating that NP–TEMP ground-state complexation can be safely ruled out. It should be noted that the efficient quenching of the



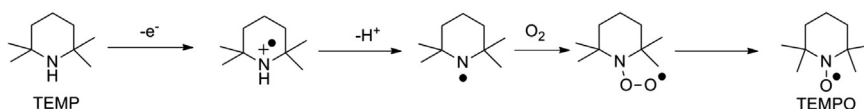


Fig. 5. Proposed mechanism for the electron transfer oxidation of TEMP to TEMPO in the presence of molecular oxygen.

singlet excited photosensitizer by TEMP and the reduced  $^1O_2$  production are not reflected in the EPR measurements of Table 1.

Overall, the results related to excited-state quenching by TEMP suggest the possibility of an alternative electron transfer reaction pathway for the oxidation of TEMP that produces a detectable TEMPO signal not involving singlet oxygen.

#### Electron transfer oxidation of TEMP to TEMPO

Photoinduced electron transfer (PET) is a feasible reaction between ketone or aromatic hydrocarbon photosensitizers and amines [26–29]. Being a secondary amine, TEMP ( $E_{ox} = 1.0$  V vs SCE) [45] could be oxidized by PET if the process is thermodynamically allowed. According to Rehm and Weller [32], this requirement is fulfilled for all the investigated photosensitizers. Indeed  $\Delta G$  for electron transfer is in all cases negative, being ca.  $-10$ ,  $-70$ ,  $-30$ , and  $-70$  kJ mol $^{-1}$  for PN, BP, NP, and CBZ, respectively.

To actually prove that an electron transfer reaction can contribute to the production of the TEMPO radical, TEMP was oxidized by BAHA (also named magic blue), a known one-electron oxidizing agent ( $E_{red} = 1.17$  V vs SCE) [46]. Addition of BAHA to a solution of TEMP in acetonitrile led to the bleaching of the initial blue color, which turned pale brown (Supplementary Fig. S7). The resulting solution was analyzed by EPR, and an enhanced TEMPO signal was observed under aerobic conditions (see Supplementary Fig. S8). The mechanistic scheme explaining these results is outlined in Fig. 5. Generation of the radical cation  $TEMP^{+\bullet}$  is followed by deprotonation and reaction of the resulting neutral radical with molecular oxygen, finally leading to the TEMPO radical [47–49].

#### The case of rose Bengal, an archetypal $^1O_2$ photosensitizer

The methodology was applied to RB, a  $^1O_2$  photosensitizer widely used in cellular experiments. Steady-state fluorescence showed an almost unaltered emission of RB singlet excited state in the presence of 100 mM TEMP (Fig. 6A). This result is in accordance with time-resolved measurements, which allowed determining a very low quenching rate constant of ca.  $10^7$  M $^{-1}$  s $^{-1}$  (Fig. 6A, inset). Likewise, the triplet excited state of RB was not affected by the presence of the secondary amine (Fig. 6B). Thus, from these data one can anticipate that the RB singlet oxygen quantum yield obtained by the TEMPO/EPR method should correlate well with that reported in the literature ( $\phi_\Delta = 0.54$ ) [50]. This was confirmed by performing the EPR experiment using PN as standard, which led to a very reasonable value of 0.56 (Fig. 6C).

#### Conclusion

Detection and quantification of singlet oxygen by means of the TEMPO/EPR method is a useful and widely employed technique. This method, however, may be misleading when the excited photosensitizer is capable of reacting with TEMP, acting as an electron donor. In this case, generation of the  $TEMP^{+\bullet}$  radical cation, followed by deprotonation and reaction with molecular oxygen, gives rise to an EPR-detectable TEMPO signal that is not associated with singlet oxygen production. The possibility of such an electron transfer interference can be anticipated by means of

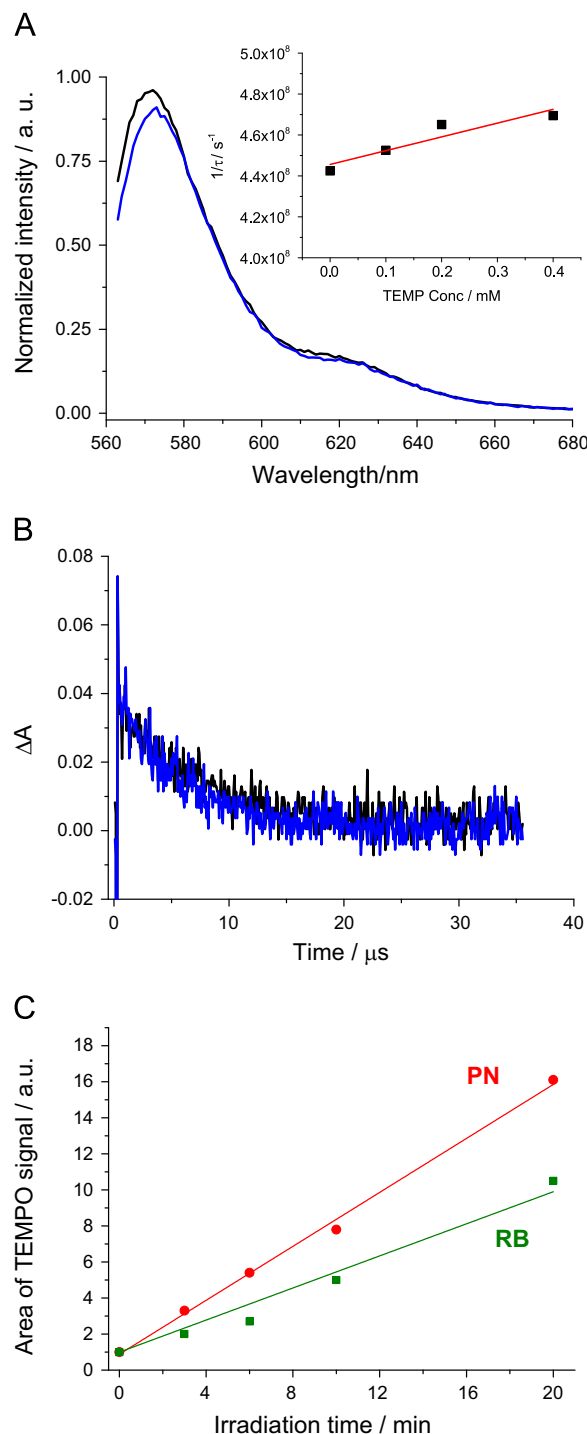


Fig. 6. (A) Emission of an aerated ACN solution of RB alone (black) or in the presence of 100 mM TEMP (blue). [RB]  $4 \times 10^{-6}$  M,  $\lambda_{ex}$  560 nm. Inset: Stern–Volmer plot obtained from time-resolved measurements of RB in the presence of increasing amounts of TEMP ( $\lambda_{ex} = 560$  nm,  $\lambda_{em} = 573$  nm). (B) Triplet–triplet absorption decays monitored at 620 nm ( $\lambda_{ex}$  532 nm) of argon-bubbled ACN solution of RB ( $3.3 \times 10^{-5}$  M) alone (black) or in the presence of 100 mM TEMP (blue). (C) Area of TEMPO signal in EPR as a function of irradiation time at 280 nm,  $A_{280}$  0.4.

simple thermodynamic calculations based on redox potentials and excited state energies. In addition, this source of artifacts can be safely ruled out when no quenching of the photosensitizer singlet and triplet excited states by TEMP is observed in fluorescence and laser flash photolysis experiments, respectively. Thus the application of such relatively simple techniques provides knowledge that is essential for an appropriate and error-free application of the TEMPO/EPR method of singlet oxygen detection in chemical, biological, and medical studies.

## Acknowledgments

The Spanish government (CTQ2012-32621, RyC-2007-00476, PFIS FI09/00312, Severo Ochoa Program SEV-2012-0267), the Carlos III Institute of Health (Grant RIRAAF, RETICS Program RD12/0013/0009), and the Generalitat Valenciana (Prometeo II/2013/005) are gratefully acknowledged for financial support. Dr. A. Vidal-Moya is acknowledged for his help with the EPR measurements.

## Appendix A. Supplementary material

Supplementary data associated with this article can be found in the online version at <http://dx.doi.org/10.1016/j.freeradbiomed.2014.08.020>.

## References

- [1] Shahidi, F.; Zhong, Y. Lipid oxidation and improving the oxidative stability. *Chem. Soc. Rev.* **39**:4067–4079; 2010.
- [2] Girotti, A. W. Translocation as a means of disseminating lipid hydroperoxide-induced oxidative damage and effector action. *Free Radic. Biol. Med.* **44**:956–968; 2008.
- [3] Hawkins, C. L.; Morgan, P. E.; Davies, M. J. Quantification of protein modification by oxidants. *Free Radic. Biol. Med.* **46**:965–988; 2009.
- [4] Jensen, R. L.; Arnbjerg, J.; Ogilby, P. R. Reaction of singlet oxygen with tryptophan in proteins: a pronounced effect of the local environment on the reaction rate. *J. Am. Chem. Soc.* **134**:9820–9826; 2012.
- [5] Pattison, D. I.; Rahmanto, A. S.; Davies, M. J. Photo-oxidation of proteins. *Photochem. Photobiol. Sci.* **11**:38–53; 2012.
- [6] Agnez-Lima, L. F.; Melo, J. T. A.; Silva, A. A.; Oliveira, A. H. S.; Timoteo, A. R. S.; Lima-Bessa, K. M.; Martinez, G. R.; Medeiros, M. H. G.; Di Mascio, P.; Galhardo, R. S.; Menck, C. F. M. DNA damage by singlet oxygen and cellular protective mechanisms. *Mutat. Res.* **751**:15–28; 2012.
- [7] Cadet, J.; Douki, T.; Ravanat, J. L. Oxidatively generated damage to the guanine moiety of DNA: mechanistic aspects and formation in cells. *Acc. Chem. Res.* **41**:1075–1083; 2008.
- [8] Cadet, J.; Douki, T.; Ravanat, J. L. Oxidatively generated base damage to cellular DNA. *Free Radic. Biol. Med.* **49**:9–21; 2010.
- [9] Lhiaubet-Vallet, V.; Miranda, M. A. Phototoxicity of drugs. In: Griesbeck, A., Lohmüller, M., Ghetti, F., editors. *CRC Handbook of Organic Photochemistry and Photobiology*. 3rd edition. Boca Raton (FL): CRC Press; 2012. p. 1541–1555.
- [10] Scheinfeld, N. S.; Chernoff, K.; Ho, M. K. D.; Liu, Y. C. Drug-induced photoallergic and phototoxic reactions—an update. *Expert Opin. Drug Saf.* **13**:321–340; 2014.
- [11] Kruff, B. I.; Greer, A. Photosensitization reactions in vitro and in vivo. *Photochem. Photobiol.* **87**:1204–1213; 2011.
- [12] Lovell, J. F.; Liu, T. W. B.; Chen, J.; Zheng, G. Activatable photosensitizers for imaging and therapy. *Chem. Rev.* **110**:2839–2857; 2010.
- [13] Schweitzer, C.; Schmidt, R. Physical mechanisms of generation and deactivation of singlet oxygen. *Chem. Rev.* **103**:1685–1758; 2003.
- [14] Baumler, W.; Regensburger, J.; Knak, A.; Felgentrager, A.; Maisch, T. UVA and endogenous photosensitizers—the detection of singlet oxygen by its luminescence. *Photochem. Photobiol. Sci.* **11**:107–117; 2012.
- [15] Ogilby, P. R. Singlet oxygen: there is indeed something new under the sun. *Chem. Soc. Rev.* **39**:3181–3209; 2010.
- [16] Lion, Y.; Delmelle, M.; Van De Vorst, A. New method of detecting singlet oxygen production. *Nature* **263**:442–443; 1976.
- [17] Burns, J.; Cooper, W.; Ferry, J.; King, D. W.; Dimento, B.; McNeill, K.; Miller, C.; Miller, W.; Peake, B.; Rusak, S.; Rose, A.; Waite, T. D. Methods for reactive oxygen species (ROS) detection in aqueous environments. *Aquat. Sci.* **74**:683–734; 2012.
- [18] He, Y.-Y.; Jiang, L.-J. Synthesis and EPR investigations of new aminated hypocrellin derivatives. *Free Radic. Biol. Med.* **28**:1642–1651; 2000.
- [19] Kladna, A.; Aboul-Enein, H. Y.; Kruk, I. Enhancing effect of melatonin on chemiluminescence accompanying decomposition of hydrogen peroxide in the presence of copper. *Free Radic. Biol. Med.* **34**:1544–1554; 2003.
- [20] Lhiaubet, V.; Paillous, N.; Chouini-Lalanne, N. Comparison of DNA damage photoinduced by ketoprofen, fenofibric acid and benzophenone via electron and energy transfer. *Photochem. Photobiol.* **74**:670–678; 2001.
- [21] Rahimipour, S.; Palivan, C.; Barbosa, F.; Bilkis, I.; Koch, Y.; Weiner, L.; Fridkin, M.; Mazur, Y.; Gescheidt, G. Chemical and photochemical electron transfer of new helianthrene derivatives: aspects of their photodynamic activity. *J. Am. Chem. Soc.* **125**:1376–1384; 2003.
- [22] Vendrell-Criado, V.; Rodríguez-Muñoz, G. M.; Cuquerella, M. C.; Lhiaubet-Vallet, V.; Miranda, M. A. Photosensitization of DNA by 5-methyl-2-pyrimidine deoxyribonucleoside: (6-4) photoproduct as a possible Trojan horse. *Angew. Chem. Int. Ed.* **52**; 2013. (6341–6341).
- [23] Yuying, H.; Jingyi, A.; Lijin, J. Effect of structural modifications on photosensitizing activities of hypocrellin dyes: EPR and spectrophotometric studies. *Free Radic. Biol. Med.* **26**:1146–1157; 1999.
- [24] Montanaro, S.; Lhiaubet-Vallet, V.; Ilesce, M.; Previtera, L.; Miranda, M. A. A mechanistic study on the phototoxicity of atorvastatin: singlet oxygen generation by a phenanthrene-like photoproduct. *Chem. Res. Toxicol.* **22**:173–178; 2008.
- [25] Nardi, G.; Lhiaubet-Vallet, V.; Leandro-Garcia, P.; Miranda, M. A. Potential phototoxicity of rosuvastatin mediated by its dihydrophenanthrene-like photoproduct. *Chem. Res. Toxicol.* **24**:1779–1785; 2011.
- [26] Cohen, S. G.; Parola, A.; Parsons, G. H. Photoreduction by amines. *Chem. Rev.* **73**:141–161; 1973.
- [27] Cossy, J.; Belotti, D. Generation of ketyl radical anions by photoinduced electron transfer (PET) between ketones and amines: synthetic applications. *Tetrahedron* **62**:6459–6470; 2006.
- [28] Turro, N. J.; Ramamurthy, V.; Scaiano, J. C. *Modern Molecular Photochemistry of Organic Molecules*. Sausalito (CA): University Sci. Books; 2010.
- [29] Yoon, U. C.; Mariano, P. S. Mechanistic and synthetic aspects of amine enone single electron-transfer photochemistry. *Acc. Chem. Res.* **25**:233–240; 1992.
- [30] Schmidt, R.; Tanielian, C.; Dunsbach, R.; Wolff, C. Phenalenone, a universal reference compound for the determination of quantum yields of singlet oxygen  $O_2(^1D_g)$  sensitization. *J. Photochem. Photobiol., A* **79**:11–17; 1994.
- [31] Barbieriková, Z.; Mihalíková, M.; Brezová, V. Photoinduced oxidation of sterically hindered amines in acetonitrile solutions and tania suspensions (an EPR study). *Photochem. Photobiol.* **88**:1442–1454; 2012.
- [32] Rehm, D.; Weller, A. Kinetics of fluorescence quenching by electron and H-atom transfer. *Isr. J. Chem.* **8**:259–271; 1970.
- [33] Wain, A. J.; Drouin, L.; Compton, R. G. Voltammetric reduction of perinaphthene in aqueous and non-aqueous media: an electrochemical ESR investigation. *J. Electroanal. Chem.* **589**:128–138; 2006.
- [34] Abad, S.; Vayá, I.; Jiménez, M. C.; Pischel, U.; Miranda, M. A. Diastereodifferentiation of novel naphthalene dyads by fluorescence quenching and excimer formation. *ChemPhysChem* **7**:2175–2183; 2006.
- [35] Limones-Herrero, D.; Pérez-Ruiz, R.; Jiménez, M. C.; Miranda, M. A. Bypassing the energy barrier of homolytic photodehalogenation in chloroaromatics through self-quenching. *Org. Lett.* **15**:1314–1317; 2013.
- [36] Oliveros, E.; Suardi-Murasecco, P.; Aminian-Saghafi, T.; Braun, A. M.; Hansen, H. -J.  $^1H$ -Phenalen-1-one: photophysical properties and singlet-oxygen production. *Helv. Chim. Acta* **74**:79–90; 1991.
- [37] Bosca, F.; Encinas, S.; Heelis, P. F.; Miranda, M. A. Photophysical and photochemical characterization of a photosensitizing drug: a combined steady state photolysis and laser flash photolysis study on carprofen. *Chem. Res. Toxicol.* **10**:820–827; 1997.
- [38] Abdel-Shafi, A. A.; Wilkinson, F. Charge transfer effects on the efficiency of singlet oxygen production following oxygen quenching of excited singlet and triplet states of aromatic hydrocarbons in acetonitrile. *J. Phys. Chem. A* **104**:5747–5757; 2000.
- [39] Darmanyan, A. P.; Foote, C. S. Solvent effects on singlet oxygen yield from  $n\pi^*$  and  $\pi\pi^*$  triplet carbonyl compounds. *J. Phys. Chem.* **97**:5032–5035; 1993.
- [40] Jensen, R. L.; Arnbjerg, J.; Ogilby, P. R. Temperature effects on the solvent-dependent deactivation of singlet oxygen. *J. Am. Chem. Soc.* **132**:8098–8105; 2010.
- [41] Zang, L.-Y.; Misra, B. R.; Van Kuijk, F. J. M. G.; Misra, H. P. EPR studies on the kinetics of quenching singlet oxygen. *Biochem. Mol. Biol. Int.* **37**:1187–1195; 1995.
- [42] Brede, O.; Beckert, D.; Windolph, C.; Göttinger, H. A. One-electron oxidation of sterically hindered amines to nitroxyl radicals: intermediate amine radical cations, aminyl,  $\alpha$ -aminoalkyl, and aminylperoxy radicals. *J. Phys. Chem. A* **102**:1457–1464; 1998.
- [43] Zhu, Q. Q.; Schnabel, W. Interaction of triplet-excited benzophenone with hindered amines and amino ethers: a laser flash photolysis study employing photoconductivity and light emission measurements. *J. Photochem. Photobiol., A* **130**:119–125; 2000.
- [44] Bortolus, P.; Monti, S.; Galiazzi, G.; Gennari, G. Complexation of aliphatic amines with carbazole in the So and S1 states: solvent effect on the deactivation of the excited complex. *Chem. Phys.* **223**:99–108; 1997.
- [45] Pischel, U.; Nau, W. M. Switch-over in photochemical reaction mechanism from hydrogen abstraction to exciplex-induced quenching: interaction of triplet-excited versus singlet-excited acetone versus cumyloxy radicals with amines. *J. Am. Chem. Soc.* **123**:9727–9737; 2001.
- [46] Ciminale, F.; Lopez, L.; Farinola, G. M.; Sportelli, S.; Nacci, A. Acid catalysis in the aminium hexachloroantimonate-induced cyclodimerization of 1-aryl-1-phenylethylenes. *Eur. J. Org. Chem.* **2002**:3850–3854; 2002.
- [47] Göttinger, H. A.; Zubarev, V. E.; Brede, O. Low-temperature EPR study of the reaction of the 2,2,6,6-tetramethylpiperidyl radical with molecular oxygen:

- direct spectroscopic observation of an aminylperoxyl radical. *J. Chem. Soc., Perkin Trans. 2*(**11**):2167–2172; 1997.
- [48] Roberts, J. R.; Ingold, K. U. Kinetic applications of electron paramagnetic resonance spectroscopy. X. Reactions of some alkylamino radicals in solution. *J. Am. Chem. Soc.* **95**:3228–3235; 1973.
- [49] Fautitano, A.; Buttafava, A.; Martinotti, F.; Bortolus, P. First electron spin resonance identification of a nitrogen peroxy radical as intermediate in the photooxidation of 2,2,6,6-tetramethylpiperidine derivatives. *J. Phys. Chem.* **88**:1187–1190; 1984.
- [50] Schmidt, R.; Afshari, E. Comment on effect of solvent on the phosphorescence rate constant of singlet molecular oxygen ( $^1\Delta_g$ ). *J. Phys. Chem.* **94**:4377–4378; 1990.